ERJ Express. Published on August 9, 2012 as doi: 10.1183/09031936.00050112

Regional lung function and heterogeneity of specific gas volume in health and emphysema

Aliverti A.[1], Pennati F. [1], Salito C.[1], Woods J.C. [2,3]

[1]TBMLab, Dipartimento di Bioingegneria, Politecnico di Milano, Milano, Italy
Departments of [2]Radiology and [3]Physics, Washington University, St. Louis, Missouri, USA;

This work was supported in part by NIH grant R01- HL090806 and Fondazione U.Veronesi.

Andrea Aliverti (ph: +39-0223999006; fax: +39-0223999000; e-mail: andrea.aliverti@polimi.it)
TBMLab, Dipartimento di Bioingegneria, Politecnico di Milano, Via G. Colombo, 40, 20133 Milano, Italy

ABSTRACT
To study regional lung function by standard CT and characterize regional variations of density and specific gas volume (SVg) between different lung volumes, we studied 10 healthy and 10 severe emphysematous subjects. Correspondent CT images taken at high and low lung volumes were registered by optical flow to obtain 2-D maps of pixel-by-pixel differences of density (ΔHU) and SVg (ΔSVg) at slice levels near the aortic arch, carina and top diaphragm.

In healthy subjects, ΔHU was higher at all levels ($p<0.001$) with higher variability expressed as interquartile range ($p<0.001$) largely due to its differences between dorsal and ventral regions. In patients, median ΔSVg values were 3.2 times lower than healthy volunteers ($p<0.001$), while heterogeneity of ΔSVg maps, expressed as quartile coefficient of variation, was 5.4 times higher ($p<0.001$). In all patients there were areas with negative values of ΔSVg.

In conclusion, ΔSVg is uniform in healthy lungs and minimally influenced by gravity. The significant ΔSVg heterogeneity observed in emphysema allows to identify areas of alveolar destruction and gas trapping and suggests that ΔSVg maps provide useful information for evaluation and planning of emerging treatments that target trapped gas for removal.

KEYWORDS
Image analysis, Emphysema, high resolution CT

INTRODUCTION

In the last few years a number of different bronchoscopic techniques have been introduced for the treatment of severe emphysema, such as airway bypass [1,2], endo-bronchial one-way exit valves [3], thermal vapor ablation [4], biological sealants [5,6], and airway implants [7]. Functional regional analysis of the lung is required as a tool for planning and guiding these treatments. Nuclear imaging, such as single photon emission tomography (SPECT) and positron emission tomography (PET), provides direct regional ventilation imaging [8-10], but suffers from low spatial resolution and low signal to noise ratio. Hyperpolarized noble gas MR imaging is a safety technique that provides regional ventilation imaging with no repeated exposure to ionizing radiationand with good temporal resolution [11-13]. Conversely, it suffers from being partially quantitative and from requiring special equipment to hyperpolarize the gas. Xenon-enhanced Computed Tomography (Xe-CT) provides a regional measure of ventilation with high spatial resolution. Xenon gas, however, is expensive, requires special equipment and must be carefully monitored because of its sedative and anesthetic properties [14,15].

Recently, standard CT has been increasingly considered not only to study parenchymal and airway wall anatomical alterations in emphysema but also to provide data on regional lung function by using images acquired at different lung volumes. Simon et al. [16] introduced the concept of specific volume change and their changes between corresponding regions at inspired and expired breath-hold CT images. Dougherty at al. [17,18] proposed an innovative method to visualize gas trapping in emphysema, based on the density changes occurring between registered lung volumes.

Coxson et al. [19] introduced the concept of specific gas volume (SVg), i.e. the volume of gas per gram of lung tissue. More recently, Salito et al. [20] demonstrated how the analysis of the variations of SVg can provide a valuable tool for clearly identifying and quantifying the extent and severity of trapped gas. The same authors have also shown [21] that the use of thick slices and a smooth filter

for image reconstruction reduce the effect of low-attenuation pixels on SVg that leads to overestimation of the severity of emphysema and trapped gas.

We hypothesized that differences in SVg obtained from registered CT images acquired at two different lung volumes, visualized as colored maps and quantified as frequency distributions, are able to provide regional functional evaluation in severe emphysema. More specifically, the aims of the present work are to: 1) introduce a new method of registration and analysis able to regionally investigate lung function in terms of SVg variations, based on standard CT images acquired at two different lung volumes; 2) evaluate the proposed method in both healthy volunteers and subjects with severe emphysema; 3) explore possible mechanisms contributing to different patterns of SVg heterogeneity, such as gravity and collateral ventilation.

MATERIALS AND METHODS

Study subjects

CT imaging on 10 healthy volunteers with no history of smoking or lung disease and on 10 patients with severe emphysema (FEV1<50%pred, RV/TLC≥0.65) were performed for this study. The Institutional Review Board of the Washington University in St. Louis approved the protocol for healthy subjects and informed written consent was obtained from each one. The data collected on emphysematous patients originated from different locations and are part of the pre-treatment assessment database of a clinical trial evaluating the safety and effectiveness of a new procedure called airway bypass (ClinicalTrials.gov Identifier: NCT00391612). Local ethical committee review and approval were obtained, and written informed consent was obtained from all the patients.

Healthy volunteers and patients were scanned while supine during suspended end-inspiration at total lung capacity (TLC) and during suspended end-expiration at residual volume (RV).

CT scans on all the healthy subjects were performed using a SOMATOM Definition Dual Source CT (DSCT; Siemens, Forchheim, Germany). Scanner settings were: tube voltage, 120 kVp; tube current, 110 mA; rotation time 500 ms; matrix 512x512; slice reconstruction thickness 5 mm. In patients with emphysema, CT imaging (rotation time 500 ms; matrix 512x512, slice reconstruction thickness 10 mm,) was performed using the same type of Siemens scanner in 9 subjects and using a GE scanner (Light-Speed VCT; GE Healthcare, Milwaukee, WI) in one patient (rotation time 741 ms). CT images were reconstructed with B30f and 'Standard' reconstruction filters, respectively for Siemens and GE scanners. The resulting radiation dose was in the order of 2.4 and 2.5-2.7 mSv per scan, respectively in healthy controls and patients.

Image analysis

The method for image segmentation, registration, and warping is summarized in Figure 1. From the scans acquired at TLC and RV, the correspondent images at the same apical-basal level of the lung

were selected. As suggested by Mishima et al. [22], three slice-levels were considered: Aortic Arch (AA), Carina (C) and Top Diaphragm (TD). At each of these levels, images taken at RV were deformed onto the TLC imagesby an automatic registration algorithm based on the optical flow method (OFM) proposed by Lucas and Kanade [23] (see below).

Successively, the inspiratory and deformed expiratory CT images were converted in both Hounsfield Units (HU) and specific gas volume (SVg) [20] and then subtracted on a pixel-by-pixel basis to evaluate the HU and SVg difference maps (ΔHU, ΔSVg) between the two lung volumes. SVg was calculated pixel-by-pixel as

$$SVg = specific\ volume_{(tissue\ and\ gas)} - specific\ volume_{(tissue)},$$

where *specific volume* (expressed in ml/g) is the inverse of density (g/ml).

The specific volume of the lung (tissue and gas) was measured from the CT as:

$$SV_{(tissue\ and\ gas)}(ml/g) = \frac{1{,}024}{HU\ (mg/ml) + 1{,}024}$$

On the basis of existing literature [24], the specific volume of tissue was assumed to be equal to 1/1.065=0.939 ml/g.

Once the maps of ΔHU and ΔSVg were obtained at AA, C and TD levels, descriptive statics was calculated.

Image registration

Image registration was performed by applying a procedure based on the following steps:

(1) segmentation of the lung, based on the method proposed by Hu et al [25];

(2) preprocessing the input images to reduce any intensity bias by extraction of the following features from the original images: Laplacian [18], external border of the lung, vessels and fissures. Laplacian was obtained by a 5-by-5 image filter approximating the shape of the two-dimensional Laplacian operator. Vessels were extracted by thresholding the images at -400 HU. Fissures were extracted semi-automatically on the basis of horizontal and vertical gradients of

the image. The extracted features were combined into a single pre-processed image satisfying the requirements of standard OFM, i.e. conservation of grey intensity of the moving structures;

(3) estimation of the global transformation describing the global motion of the lung, including translation, rotation, and dilation of the entire image;

(4) application of OFM to the pre-processed images to estimate the local deformation of the lung on a pixel-by-pixel basis. The OFM relies on the hypothesis of pixel grey intensity conservation under motion [26] and displacement vector similarity within a small neighborhood surrounding the pixel [23]. To overcome the large displacement occurring between inspiratory and expiratory lung images, a pyramidal approach [27] organized in four levels was applied. From the coarsest to the finest level of the pyramid, at each stage the motion was iteratively estimated to maximize the cross-correlation to the reference image. The resulting vector field, expressing the pixel-by-pixel displacement between the two images, was used to deform the expiratory lung image onto the inspiratory one. A linear interpolation was applied to maintain the grey-level of the parenchyma.

Quantitative Analysis

Once the registration process was completed, difference maps were obtained by subtracting Hounsfield Units and specific gas volume values pixel-by-pixel on the registered images.

Differences of Hounsfield Units (ΔHU) were defined as:

$$\Delta HU = HU\ (RV) - HU\ (TLC)$$

Differences of specific gas volume (ΔSVg), expressed in ml/g, were defined as:

$$\Delta SVg = SVg\ (TLC) - SVg\ (RV).$$

For each difference map, the corresponding frequency distribution histogram was obtained. In order to analyze the effects of gravity on the distribution of ΔHU and ΔSVg within the lung, the maps were partitioned into three gravitational regions, corresponding to thirds of the lung based on equal

vertical extent: the ventral portion, the central region, and the dorsal region. The median value of each portion is computed.

All image processing algorithms and quantitative analysis following image registration were implemented by custom software developed in MATLAB (The MathWorksInc, Natick, MA).

Statistical analysis

Statistical analysis was performed using SigmaStat version 11.0 (Systat Software, San Jose, CA).

Since frequency distributions of ΔHU and ΔSVg are not normal, descriptive statistics were performed in terms of median, interquartile range (IQR, distance between the 75th and the 25th percentile) and skewness. Quartile variation coefficient (QVC, equal to the ratio between IQR and the sum of the 75th and the 25th percentiles) was calculated and used as an index of spatial heterogeneity of ΔHU and ΔSVg distributions within the lung, with larger values indicating greater heterogeneity.

To compare median, IQR, skewness and QVC of ΔHU and ΔSVg histograms between the two groups of healthy and emphysematous subjects in the three lung levels (i.e., AA, C and TD), a two-way Analysis of Variance (ANOVA) was performed with presence of pathology and lung level as independent factors.

A two-way ANOVA was used to compare the gravitational gradient of ΔHU and ΔSVg across the lung regions (three levels: ventral, central, dorsal), with gravitational regions and lung level as independent factors.

Post-hoc tests were based on Holm-Sidak method. Significance was determined by $p<0.05$.

RESULTS

Two representative examples of the registration result are shown in Figure 2 for a healthy (a) and an emphysematous (b) subject. The registration algorithm allows in both cases to maintain the signal intensity of the original RV images and to align the main features to the TLC images.

Representative ΔHU maps are shown in Figure 3 from one healthy and one emphysematous subject. The maps at the three different considered lung levels are illustrated. In the healthy subject at each level, ΔHU is non-uniformly distributed within the lung, with increasing values from ventral to dorsal areas. In the patient with emphysema the range of ΔHU variations is markedly reduced and no gradient is present in any direction at all lung levels.

The ΔSVg maps obtained from the same subjects shown in Figure 3 are illustrated in Figure 4. While the healthy subject is characterized at every level by a homogeneous distribution of ΔSVg within the lung with ΔSVg values averaging about 5 ml/g, the patient with emphysema shows a much higher degree of ΔSVg heterogeneity and lower values averaging about 2 ml/g.

The individual histograms of ΔHU and ΔSVg of all healthy and emphysematous subjects for each lung level (shown in Fig. 5) and the results of descriptive statistics (shown in Table 1), suggest interesting observations. Clearly, ΔHU and ΔSVg heterogeneity and average values described above and shown in Figures 3 and 4 in two representative subjects were found to be common to the entire population of either healthy or emphysema. Emphysema was characterized by significantly lower median ΔHU values that were distributed over a narrower range of values (lower IQR) compared to healthy subjects ($p<0.001$). Conversely, ΔSVg was significantly lower in emphysema than in healthy subjects ($p<0.001$), and IQR was higher in emphysema than in healthy subjects ($p<0.001$). Quartile variation coefficients (QCV) of both ΔHU and ΔSVg were significantly higher ($p<0.001$) in emphysema than in healthy suggesting a higher degree of heterogeneity. Healthy subjects are also characterized by left-skewed ΔSVg histograms (i.e., longer tail in the range of lower ΔSVg values and distribution mass concentrated on the range of higher ΔSVg values)

associated to negative values of skewness, particularly at aortic arch and carina levels. This means that in the healthy lung the occurrence of high ΔSVg values is more frequent than low ΔSVg values. On the contrary, severe emphysema patients are characterized by right-skewed ΔSVg distributions and positive skewness, suggesting more frequent low ΔSVg values, independent of lung level.

The vertical (ventral to dorsal) variations of ΔHU and ΔSVg, clearly visible in the representative subjects shown in Figures 3 and 4, were quantitatively analyzed and the results are shown in Figure 6. In healthy controls ΔHU was dependent on gravity, i.e. larger in dorsal than ventral regions, at all lung levels ($p<0.01$ at AA level and $p<0.001$ at C and TD levels). This effect was more pronounced at top diaphragm level, where the central region was more significantly different than ventral ($p<0.01$) and dorsal ($p<0.001$) compared to AA and C levels. Conversely, in emphysema ΔHU, although different between levels, was not gravity dependent. No gravitational gradients of ΔSVg were present both in healthy and emphysema.

As shown by the individual ΔSVg histograms (Fig. 5), in all patients with emphysema a number of negative ΔSVg values were present. In Fig. 7 a representative example of decreasing density from TLC to RV resulting in negative ΔSVg values is shown.

DISCUSSION

In this paper we propose a new method for the analysis of the regional lung function in terms of density and specific gas volume changes between different lung volumes and we introduce innovative methods for registration of lung CT images taken at high and low lung volume. Our results demonstrate that the proposed methods can be successfully applied in both healthy subjects and patients with severe emphysema, for a qualitative and quantitative evaluation of tissue and gas changes with volume, which relate directly to lung function.

In healthy subjects, the within-subject higher variability of ΔHU values, indicated by the higher interquartile range, is associated with the gravitational dependence of density within the lung, with the dorsal regions showing values of ΔHU higher than the ventral ones (Fig. 6). Conversely, patients with severe emphysema are characterized by ΔHU values much lower than healthy controls distributed over a narrower range of values and associated with no gravity dependence (Fig. 6). When maps of ΔSVg are considered, no gravitational gradient is present both in healthy and in emphysema (Fig. 6). Healthy subjects are characterized by a homogeneous distribution of specific gas volume differences at all the three slice levels (Fig. 4, left), as indicated by the lower value of quartile variation coefficient. Conversely, specific gas volume variations are markedly lower in patients with severe emphysema and more heterogeneously distributed within the lung (Fig. 4, right). Our findings suggest that alveolar destruction and gas trapping occur at all the considered levels in the emphysematous lung with, however, a high degree of local heterogeneity and that QVC might provide an index able to detect early signs of emphysema.

Our findings are in accordance with the classical studies of Milic-Emili et al. on regional ventilation [8, 29]. These authors showed that in the range of lung volumes between 20 and 100% of vital capacity the proportion of inspired gas delivered to any lung region is constant, but gravity dependent lung zones receive relatively more of the inspired volume than the non-dependent zones.

In the current work, the ΔHU maps obtained in healthy subjects show how in the dependent (dorsal) regions gas volume changes are higher than in the non-dependent (ventral) areas. In the dependent

regions at RV density is higher as alveoli are compressed, while at TLC density is reduced by alveolar opening. Conversely, the corresponding maps of ΔSVg show that in the healthy lung ΔSVg is highly homogeneous and, therefore, the changes of the amount of gas relative to tissue mass are the same throughout the lung. The implication of these findings is that considering ΔSVg maps rather than those reported by Dougherty [17-18] or the ventilation maps proposed by Guerrero et al [30, 31], has the great advantage that the dependence of ventilation distribution on gravity is minimized. In these maps, therefore, any heterogeneity is the result of phenomena other than gravity. An interesting example is shown in Figure 4. The ΔSVg map at the TD level in the emphysema patient shows a high local heterogeneity in the ventral part of the right lung. Positive (red) and negative (blue) ΔSVg values alternate, suggesting that in this area there are small regions where SVg increases, as expected, going from RV to TLC adjacent to small regions where SVg decreases. One possible explanation of this finding is the local heterogeneity in tissue compliance. Another possible mechanism is the presence of collateral channels that allow collateral flow in this area. On the contrary, in the healthy lung collateral ventilation has a negligible importance in the distribution of ventilation as the collateral channels have about 50 times higher resistance than the normal airways [32]. Hogg et al. [32] revealed a decreased resistance to collateral airflow in the post-mortem emphysematous lung, demonstrating collateral ventilation between segments and across the major fissure. Collateral ventilation after bronchial occlusion can be studied by bronchoscopy [33-35], or by imaging techniques other than standard CT [36-38]. To the best of our knowledge, no studies in which standard CT is used to assess collateral ventilation are available.

Another representative example of how ΔSVg maps can be used to assess collateral ventilation is shown in Figure 7. In this case, showing a patient different from that shown in Figure 4, the application of a density mask (-970 HU threshold) to the corresponding images taken at TLC and RV indicates a lower amount of tissue at RV than TLC in the dorsal region. On the ΔSVg map, this corresponds to negative (blue) ΔSVg values in the same area, just below the lobar fissure. In this

example collateral ventilation seems to occur between lobes rather than within the same lobe. The general validity of the two representative cases reported above can be appreciated in Figure 5, where it is shown that all the patients show that a significant area of the histogram lies in the negative range. A possible way of quantifying the amount of collateral ventilation would be therefore to calculate the percentage of the ΔSVg histogram lying below zero in a given region.

In the present work we have also introduced a method for registration applied to CT lung images taken at different lung volumes which extends previously proposed techniques. Dougherty et al. introduced a registration algorithm to analyze density differences between different lung volumes in emphysema [39]. The same authors proposed an image pre-processing algorithm, based on the image Laplacian, to overcome the requirement of grey intensity constancy of the OFM. In this study we consider not only the image Laplacian for image pre-processing, but other features such as the external border of the lung, the vessels and the fissures, which are anatomic structures that allow more accurate registration for spatially inhomogeneous functional differences within the same slice. Our development of these algorithms was necessary to allow registration of the images taken in the healthy subjects, where density changes between high and low lung volume are so high that the Laplacian is not sufficient to satisfy the requirements of OFM.

The main limitation of this work is that the analysis was performed in 2D. This is not a difficult problem when studying emphysema, as the small lung deformation can be well tracked in two dimensions. In the healthy lung, conversely, lung deformation is much larger and this can lead to areas without corresponding vessels in the images taken at TLC and RV. This error has been partially overcome by masking the vessels thresholding the images at -400 HU both at RV and TLC. Another limitation, due to the data available from the database of the clinical trial and healthy subjects, was to consider images reconstructed with different slice thicknesses between the volunteers (5 mm) and the patients (10 mm). Nevertheless, we have recently demonstrated [21] that the disproportionate effect of low-attenuation pixels on SVg can be significantly reduced by using thick slices (5–10 mm) combined with a smooth reconstruction filter. Another possible issue in our

detailed quantitative CT analysis of severe emphysema is that accuracy of SVg is dependent on air calibration [19]. Nevertheless the methods proposed in this study are based on differences between SVg values and therefore this possible limitation is overcome. Another slight limitation is the relatively modest number of patients; all patients were characterized by severe emphysema, however, which made a homogeneous group. The obtained results demonstrate high homogeneity within the groups and high statistical significance.

The application of the present work may have important clinical and physiological implications in the assessment of different stages of disease, and in the evaluation of pharmacological or surgical treatments, such as minimally invasive interventions like trans-bronchial stents and endo-bronchial lung volume reduction. We believe that our method, once translated into clinical practice by a highly automated dedicated software, may be helpful to identify regions (lobes and/or segments) where gas trapping is more pronounced and to distinguish those patients with and without collateral ventilation and therefore who are more or less likely to benefit from lung volume reduction by minimally invasive interventions.

REFERENCES

1. Choong CK, Macklem PT, Pierce JA, Das N, Lutey BA, Martinez CO, Cooper JD. Airway bypass improves the mechanical properties of explanted emphysematous lungs. *Am J Respir Crit Care Med*. 2008; 178(9): 902-5.
2. Shah PL, Slebos DJ, Cardoso PF, Cetti E, Voelker K, Levine B, Russell ME, Goldin J, Brown M, Cooper JD, Sybrecht GW. EASE trial study group. Bronchoscopic lung-volume reduction with Exhale airway stents for emphysema (EASE trial): randomised, sham-controlled, multicentretrial. *Lancet* 2011; 378(9795): 997-1005.
3. Wan IY, Toma TP, Geddes DM, Snell G, Williams T, Venuta F, Yim AP. Bronchoscopic lung volume reduction for end-stage emphysema: report on the first 98 patients. *Chest* 2006; 129(3): 518-526.
4. Snell GI, Hopkins P, Westall G, Holsworth L, Carle A, Williams TJ.A feasibility and safety study of bronchoscopic thermal vapor ablation: a novel emphysema therapy. *Ann Thorac Surg* 2009; 88(6): 1993-1998.
5. Reilly J, Washko G, Pinto-Plata V, Velez E, Kenney L, Berger R, Celli B. Biological lung volume reduction: a new bronchoscopic therapy for advanced emphysema. *Chest* 2007; 131(4): 1108-1113.
6. Refaely Y, Dransfield M, Kramer MR, Gotfried M, Leeds W, McLennan G, Tewari S, Krasna M, Criner GJ. Biologic lung volume reduction therapy for advanced homogeneous emphysema. *Eur Respir J* 2010; 36(1): 20-27.
7. Herth FJ, Eberhard R, Gompelmann D, Slebos DJ, Ernst A. Bronchoscopic lung volume reduction with a dedicated coil: a clinical pilot study. *Ther Adv Respir Dis* 2010; 4(4): 225-231.
8. Milic-Emili J, Henderson JA, Dolovich MB, Trop D, Kaneko K. Regional distribution of inspired gas in the lung. *J ApplPhysiol*1966; 21: 749-759.

9. Bunow B, Line B, Horton M, Weiss G. Regional ventilatory clearance by xenon scintigraphy: a critical evaluation of two estimation procedures. *J Nucl Med* 1979; 20(7): 703-710.
10. Newman S, Pitcairn G, Hirst P, Rankin L. Radionuclide imaging technologies and their use in evaluating asthma drug deposition in the lung. *Adv Drug Deliv Rev* 2003; 55: 851-867.
11. Lutey BA, Lefrak SS, Woods JC, Tanoli T, Quirk JD, Bashir A, Yablonskiy DA, Conradi MS, Bartel ST, Pilgram TK, Cooper JD, Gierada DS. Hyperpolarized 3He MR imaging: physiologic monitoring observations and safety considerations in 100 consecutive subjects. *Radiology.* 2008; 248(2): 655-661.
12. Fain SB, Korosec FR, Holmes JH, O'Halloran R, Sorkness RL, Grist TM. Functional lung imaging using hyperpolarized gas MRI.*J Magn Reson Imaging* 2007; 25: 910-923.
13. Evans A, McCormack DG, Santyr G, Parraga G. Mapping and quantifying hyperpolarized 3He magnetic resonance imaging apparent diffusion coefficient gradients. *J Appl Physiol*. 2008; 105(2): 693-699.
14. Tajik JK, Tran BQ, Hoffman EA. Xenon enhanced CT imaging of local pulmonary ventilation. *Proc SPIE*1996; 2790: 40-54.
15. Marcucci C, Nyahan D, Simon BA. Distribution of pulmonary ventilation using Xe-enhanced computed tomography in prone and supine dogs. *J Appl Physiol* 2001; 90: 421-430.
16. Simon BA. Non-invasive imaging of regional lung function using x-ray computed tomography. *J Clin Monit Comput* 2000; 16: 433-42.
17. Dougherty L, Torigian DA, Affusso JD, Asmuth JC, Gefter WB. Use of an Optical Flow method for the Analysis of serial CT Lung Images. *Acad Radiol* 2006; 13: 14□23.
18. Dougherty L, Asmuth JC, Gefter WB. Alignment of CT Lung Volumes with an Optical Flow Method. *Acad Radiol* 2003; 10: 249-254.
19. Coxson HO, Rogers RM, Whittall KP, D'Yachkova Y, Paré PD, Sciurba FC, Hogg JC. A quantification of the lung surface area in emphysema using computed tomography. *Am J Respir Crit Care Med*1999; 159: 851-856.

20. Salito C, Aliverti A, Gierada DS, Deslee G, Pierce RA, Macklem PT, Woods JC. Quantification of Trapped Gas via CT and ^{3}He MRI in a New Model of Isolated Airway Obstruction. *Radiology* 2009; 253: 380-389.
21. Salito C, Woods JC, Aliverti A. Influence of CT reconstruction settings on extremely low attenuation values for specific gas volume calculation in severe emphysema. *Acad Radiol* 2011; 18(10): 1277-1284.
22. Mishima M, Itoh H, Sakai H, Nakano Y, Muro S, Hirai T, Takubo Y, Chin K, Ohi M, Nishimura K, Yamaguchi K, Nakamura T. Optimized scanning conditions of high□resolution CT in the follow□up of pulmonary emphysema. *J Comput Assist Tomogr* 1999; 23: 380□384.
23. Lucas BD, Kanade T. An iterative image registration technique with an application to stereo vision. *Proceeding of IJCAI* 1981; 81: 674-679.
24. Hedlund LW, Vock P, Effmann EL. Evaluating lung density by computed tomography. *Semin Respir Med*. 1983; 5: 76–87
25. Hu S, EA Hoffman, JM Reinhardt. Automatic lung segmentation for accurate quantification of Volumetric X□Ray CT Images. *IEEE Trans Med Imaging* 2001; 20 (6): 490-498.
26. Horn BKP, Schunck G. Determining Optical Flow. *Artificial Intelligence* 1981; 17: 185–203.
27. Beauchemin SS, Barron JL. The Computation of Optical Flow. *ACM Computing Surveys* 1995; 27 (3): 433-467.
28. Hedlund LW, Vock WP, Effmann EL. Evaluating lung density by computed tomography. *Semin Respir Med* 1983; 5: 76□87.
29. Bryan AC, Milic-Emili J, Pengelly D. Effect of gravity on the distribution of pulmonary ventilation. J Appl Physiol. 1966; 21(3): 778-84.
30. Guerrero T, Sanders K, Noyola-Martinez J, Castillo E, Zhang Y, Tapia R, Guerra R, Borghero Y, Komaki R. Quantification of regional ventilation from treatment planning CT. *Int J Radiat Oncol Biol Phys* 2005; 62: 630-634.

31. Guerrero T, Sanders K, Castillo E, Zhang Y, Bidaut L, Pan T, Komaki R. Dynamic ventilation imaging from four dimensional computed tomography. *Phys Med Biol* 2006; 51: 777□791

32. Hogg JC, Macklem PT, Thurlbeck WM. The resistance of collateral channels in excised human lungs. *J Clin Invest* 1969; 48: 421-431.

33. Terry PB, Traystman RJ, Newball HH. Collateral ventilation in man. *N Engl J Med* 1978; 298: 10-15.

34. Morrell NW, Wignall BK, Biggs T, Seed WA. Collateral ventilation and gas exchange in emphysema. *Am J Respir Crit Care Med* 1994; 150: 635-641.

35. Aljuri N, Freitag L. Validation and pilot clinical study of a new bronchoscopic method to measure collateral ventilation before endobronchial lung volume reduction. *J ApplPhysiol*2009; 106: 774-783.

36. Salanitri J, Kalff V, Kelly M, HolsworthL, Williams T, Snell G. ^{133}Xenon ventilation scintigraphy applied to bronchoscopic lung volume reduction techniques for emphysema: relevance of interlobar collaterals. *Intern Med J* 2005; 35: 97-103.

37. Bartel SE, Haywood SE, Woods JC, Chang YV, Menard C, Yablonskiy DA, Gierada DS, Conradi MS. Role of collateral paths in long-range diffusion in lungs. *J Appl Physiol*. 2008; 104(5): 1495-503.

38. Woods JC, Choong CK, Yablonskiy DA, Bentley J, Wong J, Pierce JA, Cooper JD, Macklem PT, Conradi MS, Hogg JC. Hyperpolarized 3He diffusion MRI and histology in pulmonary emphysema. *Magn Reson Med*. 2006; 56(6): 1293-300.

39. Torigian DA, Gefter WB, Affuso JD, Emami K, Dougherty L. Application of an optical flow method to inspiratory and expiratory lung MDCT to assess regional air trapping: a feasibility study. *AJR Am J Roentgenol*. 2007; 188(3): W276-80.

FIGURE LEGEND

Fig.1

Schematic diagram of the proposed method for the analysis of regional distribution of specific gas volume changes between Total Lung Capacity (TLC) and Residual Volume (RV). Two corresponding slices acquired at TLC and RV on the same lung level are firstly segmented and pre-processed to extract the relevant features (see text). The pre-processed images are then registered by the optical flow technique. The resulting deformation field is applied to the original segmented RV image to warp it onto the reference (TLC image). The original TLC and the deformed RV images are then converted into SVg images and subtracted pixel-by-pixel, to obtain ΔSVg colored maps.

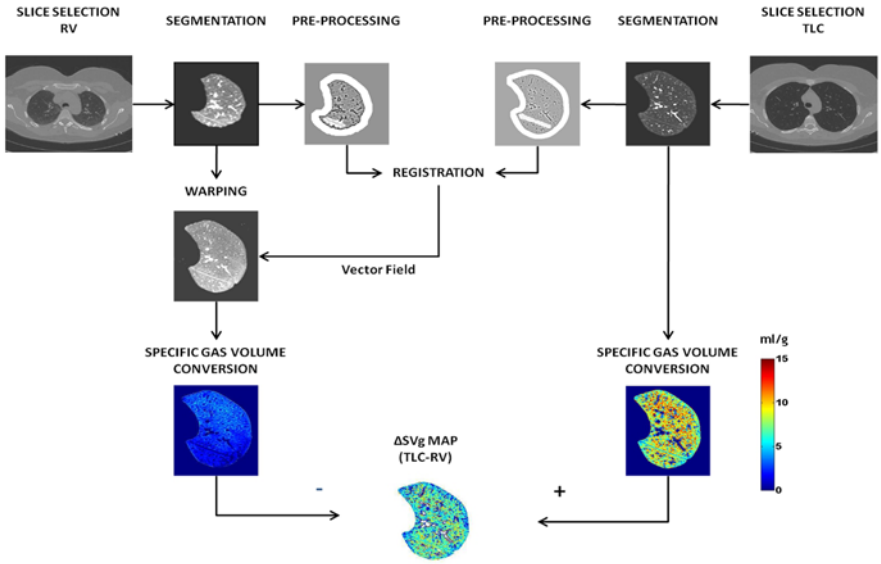

Fig. 2

Representative results of image registration process on healthy (a) and emphysematous (b) lungs. On each panel, the segmented lung at residual volume (RV, left), total lung capacity (TLC, center), and the deformed RV image (registered RV, right) are shown.

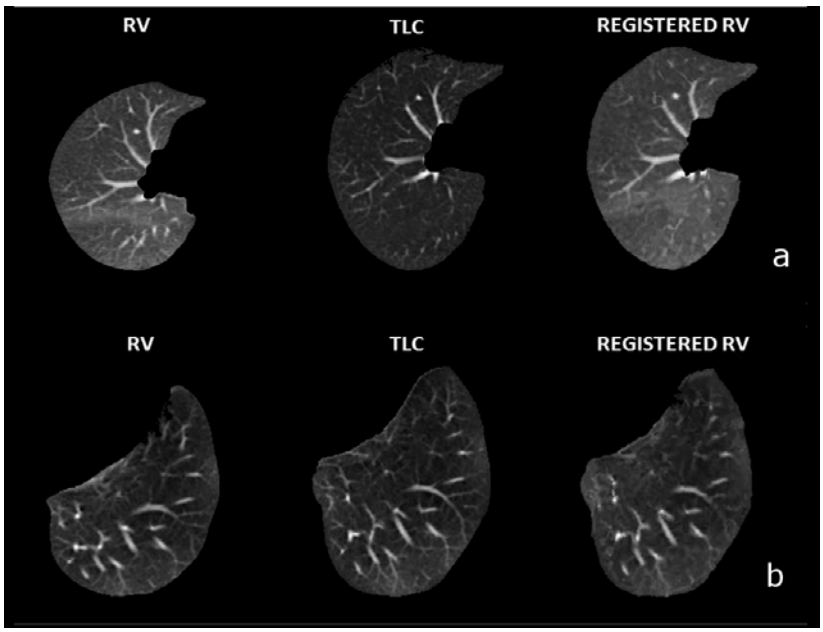

Fig. 3

HU variations, computed as $\Delta HU=HU_{WARPED\ RV}-HU_{TLC}$ of a representative healthy and emphysematous subject, calculated at aortic arch (AA), carina (C) and above diaphragm (TD) levels. The ranges of display are chosen differently for the two groups (-100 to 300 HU for the healthy and -100 to 100 HU for the emphysematous lung) in order to highlight the changes occurring between the two lung volumes in emphysema, which is characterized by a lower range of variation.

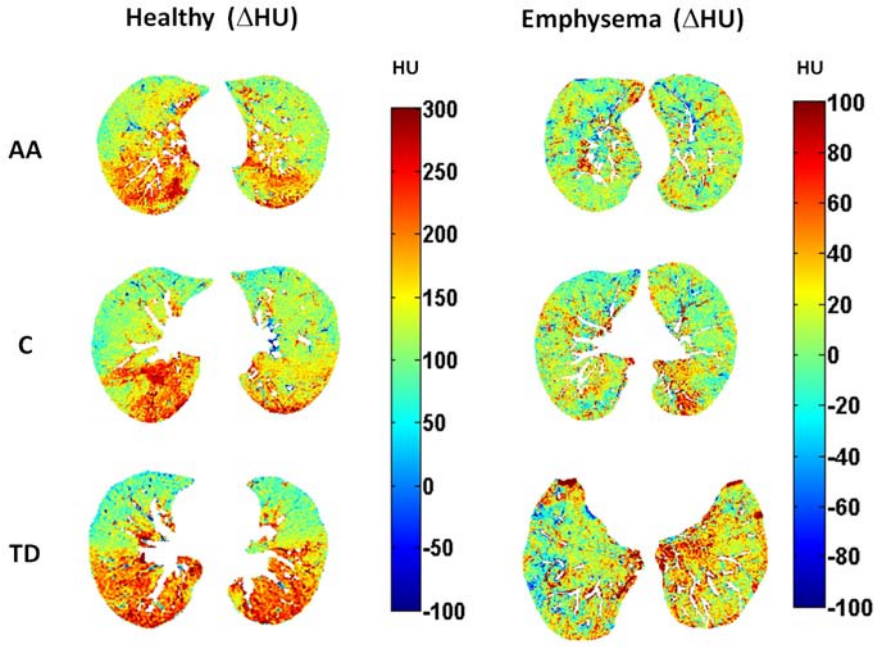

Fig. 4

SVg difference maps ($\Delta SVg = SVg_{TLC} - SVg_{WARPED\ RV}$) of a representative healthy and emphysematous subject, calculated at aortic arch (AA), carina (C) and above diaphragm (TD) levels. The chosen range of display is from -10 to 10 ml/g in both the cases.

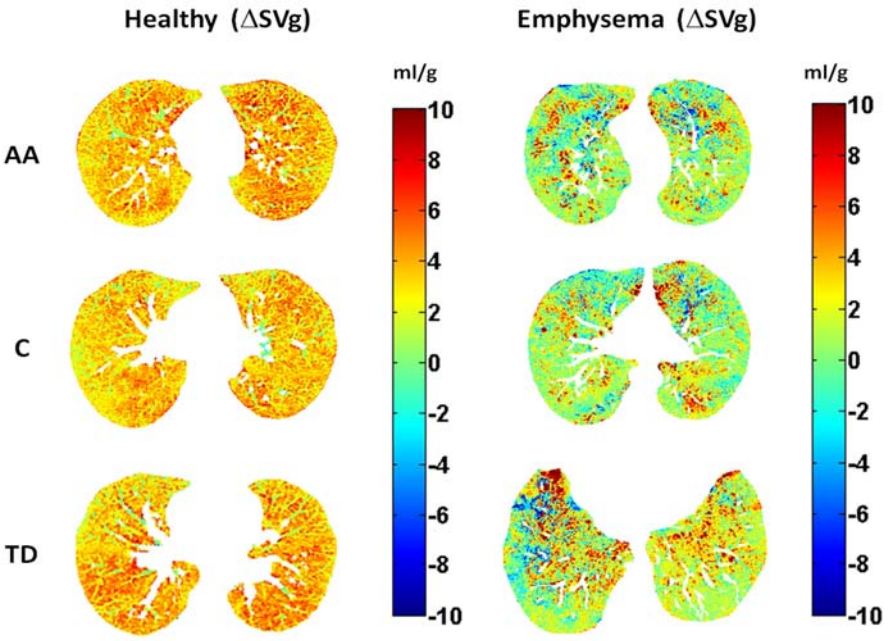

Fig. 5

Probability distribution of ΔHU and ΔSVg values of the three levels of the lung. In each graph, The healthy (reported in blue), are characterized by higher ΔHU and ΔSVg values, as the histograms are shifted towards higher values. The interquartile range of the healthy results higher in ΔHU but lower in ΔSVg in respect to emphysema, and this behavior could be explained by the gravity effect to which the healthy maps are subjected. Moreover, in emphysema these histograms show a variable percentage of negative values, that could be explained as a different percentage of collateral ventilation.

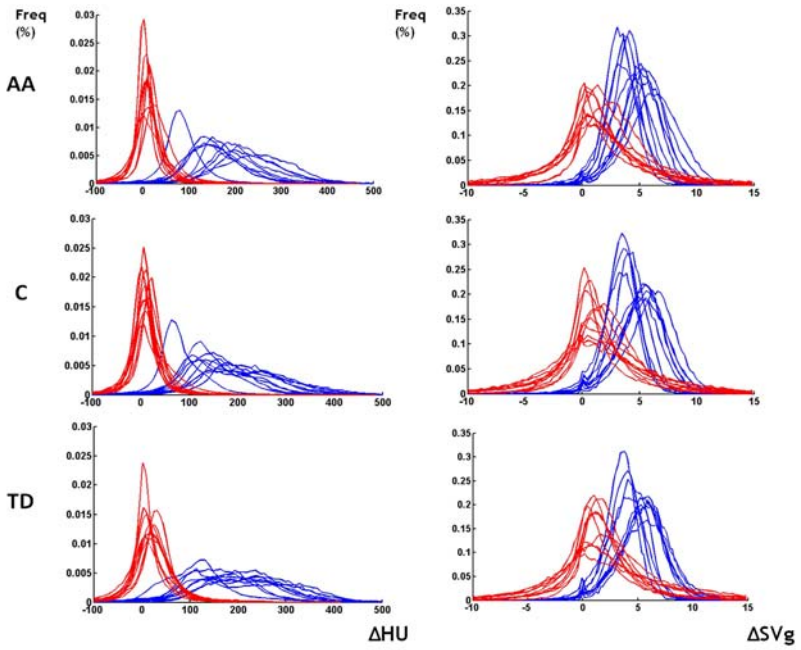

Fig. 6

Gravity dependence of ΔHU (top panels) and ΔSVg (bottom panels) in healthy controls (left panels) and emphysematous subjects (right panels). In each panel the median values of ventral, central and dorsal portions of the lung at aortic arch (AA), carina (C) and top diaphragm (TD) levels are shown. *: p<0.05; **: p<0.01; ***: p<0.001

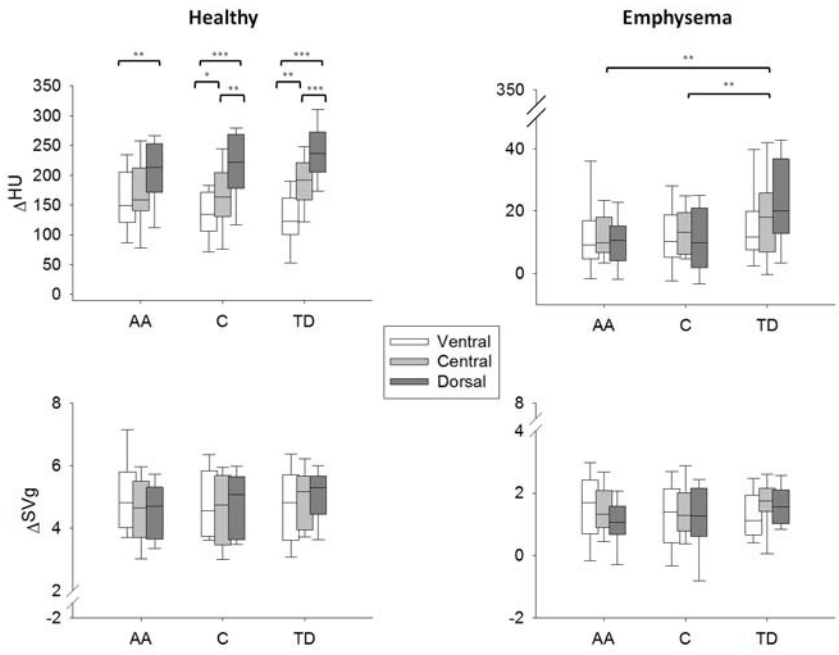

Fig.7

Example of inter-lobar collateral ventilation assessed by standard CT. We applied a density mask to correspondent images at TLC and RV highlighting the pixels below -970 HU: a decrease in density from TLC to RV is clearly visible. The areas where this phenomena happens (as the one indicated by the arrows), result in negative ΔSVg values, shown as blue areas.

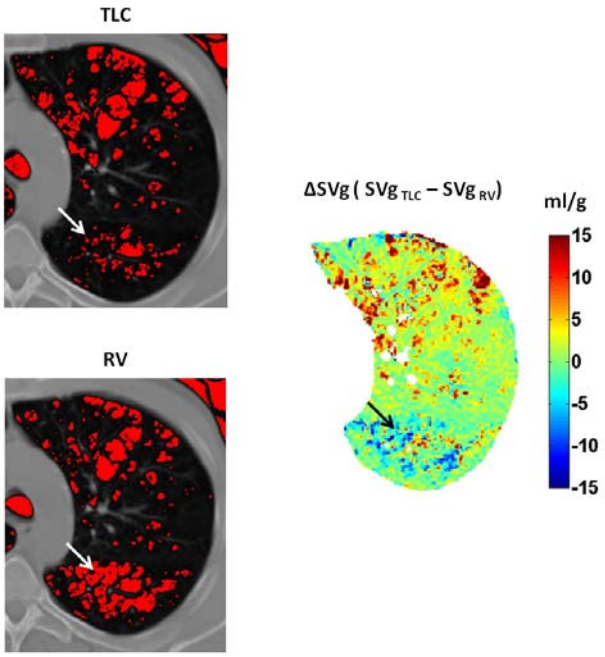

Table 1 – Descriptive statistics of ΔHU ($\Delta HU = HU_{WARPED\ RV} - HU_{TLC}$) and ΔSVg($\Delta SVg = SVg_{TLC} - SVg_{WARPED\ RV}$) values. Average values of median, interquartile range (IQR), skewness and quartile coefficient variation (QCV) of all healthy and emphysematous subjects are reported, at aortic arch (AA), carina (C) and above diaphragm (TD). ***: $p<0.001$ (vs corresponding healthy average).

**: $p<0.01$(vs corresponding healthy average).

	ΔHU (HU)						**ΔSVg (ml/g)**					
	Healthy			**Emphysema**			**Healthy**			**Emphysema**		
	AA	**C**	**TD**	**AA**	**C**	**TD**	**AA**	**C**	**TD**	**AA**	**C**	**TD**
Median	176±50	168±46	192±38	12,5±7,6***	12±6***	19±9***	4,7±1,0	4,7±1,0	4,9±0,9	1,3±0,6***	1,3±0,6***	1,5±0,5***
IQR	80±16	97±24	118±25	33,3±9,1***	34±10***	43±8***	2,2±0,4	2,3±0,4	2,5±0,4	4,0±0,8***	4,1±1,2***	4,1±1,5***
Skewness	-0,2±0,4	-0,0±0,3	-0,1±0,2	0,0±0,7	-0,1±1,1	-0,1±0,5	-0,2±0,4	-0,1±0,4	-0,003±0,3	0,5±0,5***	0,6±0,5**	0,6±0,3***
QCV	0,2±0,03	0,3±0,04	0,3±0,0	1,5±0,6***	1,7±1,0***	1,2±0,5***	0,2±0,04	0,3±0,04	0,3±0,03	1,5±0,6***	1,6±0,9***	1,2±0,5***